Science Advances
AAAS

advances.sciencemag.org/cgi/content/full/6/10/eaax1909/DC1

Supplementary Materials for

Nanoscale integrin cluster dynamics controls cellular mechanosensing via FAKY397 phosphorylation

Bo Cheng, Wanting Wan, Guoyou Huang, Yuhui Li, Guy M. Genin, Mohammad R. K. Mofrad, Tian Jian Lu, Feng Xu, Min Lin*

*Corresponding author. Email: minlin@mail.xjtu.edu.cn

Published 4 March 2020, *Sci. Adv.* **6**, eaax1909 (2020)
DOI: 10.1126/sciadv.aax1909

This PDF file includes:

Note S1. The ordinary differential equations for integrin clustering, cluster disassembly, and FAKY397 activation.

1.1 Conservation equations

To reduce the computational complexity of the model and ensure stability of the numerical solution, we ensured that the total quantity of each protein species in the simulation did not change. The initial quantity of each active protein was 1% of the total, and the corresponding inactive protein could be calculated from conservation equations (**Table S3**).

1.2 Descriptions of chemical reactions

The 24 types of integrins in mammals are comprised of 18 types of α-subunit and 8 types of β-subunit (*Moreno-Layseca et al., Nature Cell Biology, 2019*). $\alpha_5\beta_1$ integrins and $\alpha_v\beta_3$ integrins play key roles in cell-adhesion dynamics. The integrins can be activated by talin in what is often termed “inside-out” activation. The activation rate of $\alpha_v\beta_3$ integrin is larger than that of $\alpha_5\beta_1$ integrin. Active integrins can be clustered by other molecules (*e.g.*, $PI(4,5)P_2$ and kindlin2) or integrin transmembrane domains (ITDs) (*Calderwood et al., Nature Reviews Molecular Cell Biology, 2013*). Clustered β_3 integrins can activate Src by inducing Tyr-418 phosphorylation of Src, while clustered β_1 integrins can activate FAK by inducing Tyr-397 phosphorylation of FAK (*Schroer et al., Cellular and Molecular Bioengineering, 2013*). Equations describing integrin activation and clustering are listed in **Table S4**.

According to our spatial Monte Carlo models, we used following functions to represent the contract units (CUs) and stiffness mediated cluster assembly

$$L = \begin{cases} 2t & t < 30s \\ 60 & t \geq 30\text{s} \end{cases} \quad \text{(S1)}$$

$$k_{3f\ (4f)} = 0.01 \frac{k_{int} k_{ecm}}{k_{int} + k_{ecm}} L \quad \text{(S2)}$$

where L is the CU-mediated displacement (nm); k_{int} and k_{ecm} are the stiffness (pN/nm) for integrin and substrate, respectively. Thus, k_{3f} and k_{4f} represent the stiffness/force-mediated integrin binding rates (s^{-1}). Kank-mediated cluster disassembly is described as follows

$$k_{3r} = 0.03e^{\gamma t} \quad \text{(S3)}$$

$$k_{4r} = 0.01e^{\gamma t} \quad \text{(S4)}$$

where γ is an adjustable factor representing the Kank binding rate (s^{-1}). Thus, k_{3f} and k_{4f} (s^{-1}) represent the increase of the time-dependent effective off rate as induced by Kank binding. Note that this exponential function is consistent with our Monte Carlo simulation results.

The FAK-Src complex is an important dual kinase complex (*Mitra et al., Current Opinion in Cell Biology, 2006*). The FAK-Src complex can activate various proteins such as p130Cas and paxillin. The phosphorylated tyrosine 397 of FAK can bind with SH2 domain of Src that inhibits deactivation of phosphorylation of tyrosine 527 of Src, then leading to an increase of Src activity. The activated Src in turn can cause phosphorylation of FAK at tyrosines at 925, 576 and 577, resulting in a full activation of FAK. Thus, FAK and Src each have three states in our model, *i.e.*, inactive (Src_ina and FAK_ina), partially active (Src_p and FAK_p) and full active (Src_3p and FAK_3p) (**Table S4**).

1.3 pPaxillin/FAK mediated negative feedback regulation

Based on the negative feedback regulation described the Materials and Methods section, we added a pPaxillin/FAK mediated negative feedback loop to the ODE-model (*Zaidel-Bar et al., Journal of Cell Science, 2007*). Note that, in this expanded ODE-model, we used negative feedback regulation, but not Kank dynamics, to promote the cluster disassembly (**Table S5**).

Note S2. Assumptions.

2.1 The molecular mechanisms of integrin clustering dynamics

Integrins are transmembrane molecules with large extracellular domains that bind to ECM and with small intracellular tails that interact with adhesion molecules. A great diversity of opinion exists about how integrins might cluster. We focused on three

specific mechanisms in our model amongst the many hypotheses in the literature, for the reasons listed below:

(1) ITD-mediated integrin clustering

Existing studies support the hypothesis that integrins connect noncovalently via their ITDs. Using electron cryomicroscopy and single particle image reconstruction, Adair *et al.* observed that $\alpha_{IIb}\beta_3$ integrins can form a heterodimer via ITD interactions (*Adair et al., PNAS, 2002*). Li *et al.* used two mutations of $\alpha_{IIb}\beta_3$ integrin to show that the α-subunits of $\alpha_{IIb}\beta_3$ integrin tend to form homodimers, while β-subunits tend to form homotrimers (*Li et al., Science, 2003*). Li *et al.* also found that purified wild-type $\alpha_{IIb}\beta_3$ integrins tend to form dimers and trimers *in vitro* when integrins are activated by Mn^{2+} (*Li et al., Science, 2003*). Gottschalk *et al.* used a computational approach to show that $\alpha_{IIb}\beta_3$ integrins can form stable α_{IIb} homodimers and β_3 homotrimers by forming a GpA-like conformation (*Gottschalk et al., Structure, 2004*).

Luo *et al.* further suggested that β3G708N mutation of $\alpha_{IIb}\beta_3$ integrin enhances integrin-FN affinity but does not influence the integrin clustering, as experimentally observed via confocal microscopy, thus excluding ITD interaction mediated integrin clustering (*Luo et al., PNAS, 2005*). However, because it is still difficult to directly observe the high-resolution structures of ITD-interaction *in vivo*, we chose not to rule out IDT-mediated integrin lateral clustering to occur as one of the potential mechanisms of integrin

clustering in our model. Integrin molecules were coarse-grained in our model as 10 nm diameter circles, without distinguishing the α and β subunits. Because ITD-interaction mediated clustering can happen through direct contact, we thus applied a chemical reaction rate equation to represent integrin clustering when the distance between the circles representing two integrin molecules dropped below 15 nm.

(2) PI(4,5)P2 mediated integrin clustering

Caroline *et al.* showed that integrin clustering requires lateral interactions of talin-integrin complexes and lipid raft domains containing PI(4,5)P2 (*Caroline et al., Journal of Cell Biolog, 2005*). Interestingly, Wei *et al.* also showed that active β_1 integrins are localized with lipid rafts (*Wei et al., American Journal of Physiology Cell Physiology, 2008*). Inhibition of lipid rafts will decrease integrin activation and FAKY397 phosphorylation. Leitinger *et al.* also showed that lymphocyte function-associated antigen (LFA-1) and $\alpha_4\beta_1$ integrin clustering requires intact lipid raft structures (*Leitinger et al., Journal of Cell Science, 2002*). Although lipid raft domains play important roles in integrin clustering, the molecular mechanisms remain unclear. Because integrin-PIP2 molecule interactions in lipid raft domain will decrease the diffusion rate of integrin molecules, we studied several lipid raft domains with integrins having a lower diffusion rate and thereby evaluated the effects of lipid raft domains on integrin clustering.

(3) Integrin-crosstalk mediated integrin clustering

Ye *et al.* reported the possibility of activated integrin activating surrounding inactive integrins by ITD interactions (*Ye et al., Journal of Biological Chemistry, 2014*). This experimental observation provides a potential molecular mechanism for positive feedback regulation between integrin activation and clustering. Thus, in our integrin clustering sub-model, we used a scalable "integrin-crosstalk parameter" to investigate effects that positive feedback would have on integrin clustering.

2.2 Assessment of the assumption of a homogenous tension/strain distribution amongst integrin molecules within integrin clusters

To assess the degree to which different distributions of tension or strain within clusters might affect our model predictions, we compared our model to the molecular clutch model developed by Odde and co-workers (*Chan et al., Science, 2008*) which has unequal molecular force distributions. In the model of Odde, *et al.*, the lengths of connected integrins within adhesions are different, resulting an unequal force distribution over the integrin molecules; while in our model, the lengths of connected integrins in adhesions are equal, resulting in an equal force distribution over the integrin molecules.

We performed a simulation using these two models based on the same initial conditions, including the same number of clutches, the same binding-unbinding rate and the same displacement boundary condition. Comparing the results from the two models (**Fig. S4**)

revealed that, in the model of Odde, *et al*., integrin cluster lifetime decreases with increasing substrate stiffness, consistent with how nerve cells produce stronger tractions and adhesions on softer substrata. Our model, however, predicts that cluster lifetime increases with increasing substrate stiffness, consistent experimental observations for 3T3 fibroblasts. We therefore believe that different forces distributions exist for different cell types. Because we focused on 3T3, MDCK and HT1080 cells for our experiments, we therefore used an equal force distribution across integrin molecules in our model.

2.3 Kank-mediated cluster disassembly

Kank can mediate the disassembly of clusters, by action at the periphery of clusters. However, this spatially-dependent action of Kank led to substantial reduction in the computational efficiency of our model. We therefore evaluated whether a spatially-independent model of Kank action could be used. Upon finding predictions of the two models were within a few percent of one another, we adopted the spatially-independent model for all subsequent computations.

These Kank-mediated cluster disassembly models were studied using the whole cell simulation: in one model, Kanks were distributed uniformly within an intact focal adhesion containing multiple clusters; in the other, Kanks were localized to the periphery the adhesion (Figs. S5A, B). The sliding rates of the adhesion for the two models,

characterized by the time history of the position of the centroid of the clusters, were indistinguishable (Figs. S5D-E).

Note S3. Limitations and potential problems.

3.1 The turnover rates of integrin and adaptor proteins

Integrins and adaptor proteins can change turnover rates in response to FAKY397 phosphorylation. We emphasize that these effects were omitted from the model to ensure simplicity. Thus, we assumed that adaptors can form a stable composite platform connecting the actin cytoskeleton with integrins. However, simulations containing distinct dynamics of integrin and other adaptor proteins represent an important possible extension of this work.

3.2 Other potential integrin clustering mechanisms

In addition to the three mechanisms that are incorporated into our model, other potential clustering mechanisms have been proposed. These include a talin/PIP2/PIPKIγ signaling loop, Kindlin-PIP2 complexes, interactions with the cortical actin cytoskeleton, molecular partner-switching, and mechanical resistance from the glycocalyx. Some of the mechanisms we modeled might act in parallel with these mechanisms, and any of these mechanisms might someday be shown to be inconsequential or fictional. We acknowledge that the mechanisms we modeled represent our current bias amongst the

many possible mechanisms, and briefly describe below the several potentially viable mechanisms that we neglected.

(i) The talin/PIP2/PIPKIγ positive feedback loop

The talin/PIP2/PIPKIγ signaling loop has been shown to initiate integrin clustering (*Ling et al., Journal of Cell Biology, 2003*). In this loop, PIP2 binds with talin, linking integrins into clusters, but does so in competition with PIPKIγ. Binding of PIPKIγ to talin thereby competitively reduces integrin activation and integrin clustering by filling the spaces needed by PIP2.

(ii) Kindlin mediated integrin clustering

Dimeric kindlin might also promote integrin clustering (*Li et al., PNAS, 2017*). However, its putative action remains controversial because the mechanism of monomer-dimer transition of kindlins is still unclear. One hypothesized molecular mechanism is that kindlin could form dimeric kindlin with anionic phospholipids on the membrane. The support for this hypothesis is that phosphoinositide membrane-binding sites have be found in F0-F1 and PH domains of kindlin (*Liu et al., Journal of Biological Chemistry, 2011*).

(iii) Interactions with the cortical actin cytoskeleton

The cortical actin cytoskeleton might provide diffusion barriers to promote integrin

clustering. By sequestering integrin molecules into corrals, the chance of integrins encountering one another can be increased. However, working against this mechanism is the problem that because integrin diffusion is restricted by the actin cortex, the lateral assembly of integrins might also be attenuated by this mechanism.

(iv) Partner-switching

The partner-switching process can also promote integrin clustering (*Woolf et al., Biophysical Chemistry, 2003*). Partner-switching means that each integrin can bind with any neighboring integrin. If the integrin binding and unbinding rate is larger than the diffusion rate, then integrin can share bonds between multiple integrins, resulting in clusters other than dimers.

(v) Mechanical resistance from the glycocalyx

The mechanical resistance produced by a glycocalyx layer located at interface between plasma membrane and substrate has been shown to relate to integrin clustering (*Paszek et al., Nature, 2014*). Models based on this putative mechanism can describe how integrin area (size) relates to stiffness.

3.3 The distance between molecules for integrin clustering

Our focus is a handful of what are certainly many redundant mechanisms for integrin cluster formation. Work of the Spatz group (*Beer et al., PRE, 2010*) shows that

mechanosensing is possible on substrata with integrin receptors spaced 50 nm apart, far longer than the 10-20 nm lengthscale of PIP_2 and ITD mediated clustering. This suggests that other putative linkers such as talin, kindlin or α-actinin (up to 70 nm) might be capable of forming clusters as well.

3.4 The assembly processes of ECM proteins

Fibronectins assemble into a fibrillar structure in vivo, which will influence integrin-ECM interaction significantly. Integrin in clusters can activate FAK and the activated FAK can recruit Src to form a signal complex. Such a signal complex can activate the Rho GTPases which then promote organization of actin cytoskeleton to sustain the intracellular tension. The intracellular tension can expand and unfold the FN dimers to promote the FN-FN interaction and then initiating the FN fibril formation. FN assembly can provide more integrin binding sites and further increase the integrin binding rate (*Wierzbicka-Patynowski et al., Journal of Cell Science, 2003; Weinberg et al., Biophysical Journal, 2017*). However, adding the fibril assembly process into our simulation will greatly increase the complexity and computational cost of the model. For simplicity, we did not consider the fibril assembly process in our model. However, coupling the assembly dynamics and steric presentation of binding sites represents an important direction for future studies.

Note S4. Quantified relationship between substrate stiffness and FAKY397 phosphorylation.

The simulation consists of three processes: integrin cluster formation on the plasma membrane, stiffness-dependent disassembly of integrin cluster and FAKY397 phosphorylation within integrin clusters. Integrin clustering dynamics is modeled by a spatial Monte Carlo model. The size distribution of integrin clusters obeys a power distribution in agreement with the experimental results (**Eq. 2**). Then, a stretchable parallel spring model is used to investigate the effect of the substrate stiffness on the lifetime of integrin clusters. The relationship between clustered integrin number and substrate stiffness fits a simple Hill function well (**Eq. 3**). The size distribution and lifetime of integrin clusters are two important elements (inputs of particle-based simulation) to determine the reaction rate and time of FAKY397 phosphorylation. Therefore, a spatially particle-based simulation is used to study the effect of clustered integrin number on the FAKY397 phosphorylation. The number of FAKpY397 linearly increases with clustered integrin number (**Eq. 4**). Finally, a simple algebraic expression is gotten to describe the stiffness-dependent mechanochemical conversion processes, *i.e.*, the relationship between substrate stiffness and FAKpY397 number (**Eq. 5**). Integrin density, FAK molecules in the cytoplasm and diffusion constant can mostly influence the different mechanosensing behaviors for different types of cells.

Table S1. The plasma membrane events and transition rates.

Events	Transition rates	Base rates	Range
Translational diffusion	$\sigma_{i\to j}^{D} = \frac{1}{6}\sigma^{D}\tau_i(1-\tau_j)$ τ_i is the occupancy function that is 1, if site i is filled, and 0, if site i is empty. D_d is the diffusivity of single integrin molecule or integrin polymer. a is the lattice pixel dimension.	D_d = 0.01 μm^2/s; a = 15 nm;	D_d = 0.005~0.02 μm^2/s
Integrin activation by talin (inactive integrin → active integrin)	$\sigma_i^R = k_{a+}[C_{talin}]\tau_i$	k_{a+} = 0.3 s^{-1} ;	k_{a+} = 0.03~3 s^{-1} ;
Integrin inactivation (active integrin → inactive integrin)	$\sigma_i^R = k_{a-}\tau_i$	k_{a-} = 0.1 s^{-1} ;	k_{a-} = 0.01~1 s^{-1} ;
Integrin clustering	$\sigma_i^R = \frac{k_{c+}[C_{PIP2}]}{6}\tau_i\tau_j$, $\sigma_i^R = \frac{k_{d+}[C_{rods}]}{6}\tau_i\tau_j$	k_{c+} = k_{d+} = 1 (receptors/sites)$^{-1}$ s^{-1};	k_{c+} = k_{d+} = 0.1~10 (receptors/sites)$^{-1}$ s^{-1} ;
Integrin cluster disassembly	$\sigma_i^R = k_{c-}\tau_i\tau_j$, $\sigma_i^R = k_{d-}\tau_i\tau_j$	k_{c-} = k_{d-} =0.1 s^{-1} ;	k_{c-} = k_{d-} = 0.01~1 s^{-1} ;

Table S2. Baseline model parameters.

Parameter	Symbol	Value
Integrin molecule number in the simulation	N_i	500
The based time required to form an integrin cluster	t_{exp}	40 s
Integrin cluster displacement rate	ΔL	3 nm/s
Integrin cluster maximum displacement	L_{max}	60 nm
Catch-slip bond parameters	k_a	0.004 s^{-1}
	k_b	10 s^{-1}
	F_a	15 pN
	F_b	15 pN
The stiffness of integrin	k_{int}	1 pN/nm
The stiffness of ECM	k_{ecm}	0.01 ~ 100 kPa
Activations rate of $\alpha_v\beta_3$ integrin	*k1f*	23 s^{-1}
Deactivations rate of $\alpha_v\beta_3$ integrin	*k1r*	0.576 s^{-1}
Activations rate of $\alpha_5\beta_1$ integrin	*k2f*	23 s^{-1}
Deactivations rate of $\alpha_5\beta_1$ integrin	*k2r*	0.576 s^{-1}
Cluster assembly rate of $\alpha_v\beta_3$ integrin	*k3f*	1 s^{-1}
Cluster disassembly rate of $\alpha_v\beta_3$ integrin	*k3r*	0.1 s^{-1}
Cluster assembly rate of $\alpha_5\beta_1$ integrin	*k4f*	1 s^{-1}
Cluster disassembly rate of $\alpha_5\beta_1$ integrin	*k4r*	0.1 s^{-1}
pPaxillin mediated $\alpha_v\beta_3$ integrin assembly rate	*k3f_p*	0.1 s^{-1}
pPaxillin/FAK mediated $\alpha_v\beta_3$ integrin disassembly rate	*k3r_p*	1 s^{-1}

pPaxillin mediated $\alpha_5\beta_1$ integrin assembly rate	*k4f_p*	0.1 s^{-1}
pPaxillin/FAK mediated $\alpha_5\beta_1$ integrin disassembly rate	*k4r_p*	1 s^{-1}
Src base autophosphorylation rate	*k5f0*	0.1 s^{-1}
Integrin-mediated autophosphorylation rate of Src	*k5f*	0.454 s^{-1}
Dephosphorylation rate of pSrc	*k5r*	432 s^{-1}
FAK-mediated pSrc phosphorylation rate	*k6f0*	29 s^{-1}
Dephosphorylation rate of 3pSrc	*k6r*	432 s^{-1}
FAK base autophosphorylation rate	*k7f0*	0.1 s^{-1}
Integrin-mediated autophosphorylation rate of FAK	*k7f*	20.15 s^{-1}
Dephosphorylation rate of pFAK	*k7r*	48 s^{-1}
Src-mediated pFAK phosphorylation rate	*k8f*	29 s^{-1}
Dephosphorylation of 3pFAK	*k8r*	48 s^{-1}
Paxillin activation rate	*k10f*	1 s^{-1}
Disassembly rate of pPaxillin/FAK complex	*k10r*	2 s^{-1}
pPaxillin/FAK complex formation rate	*k9f*	1 s^{-1}
Disassembly of pPaxillin/FAK complex rate	*k9r*	2 s^{-1}

Table S3. Conservation equations.

Protein type	Mass conservation equation
$\alpha_v\beta_3$ integrin	IV3_integrin_tot = IV3_integrin_ina + IV3_integrin_a + IV3_integrin_clu
$\alpha_5\beta_1$ integrin	I51_integrin_tot = I51_integrin_ina + I51_integrin_a + I51_integrin_clu
Src	Src_tot = Src_ina + Src_p + Src_3p
FAK	FAK_tot = FAK_ina + FAK_p + FAK_3p + Pxillin_FAK
Paxillin	Paxillin_tot = Paxillin_ina + Paxillin_p + Paxillin_FAK

Table S4. Equations describing integrin activation and clustering and FAK-Src interactions.

$\alpha_v\beta_3$ integrin Description	Chemical Equations
$\alpha_v\beta_3$ integrin activation	IV3_integin_on_rate = k1f * IV3_integrin_ina
$\alpha_v\beta_3$ integrin deactivation	IV3_integin_off_rate = - k1r * IV3_integrin_a
$\alpha_v\beta_3$ integrin cluster assembly	IV3_integin_on_clu_rate = (k3f + Paxillin_p * k3f_p) * IV3_integrin_a
$\alpha_v\beta_3$ integrin cluster disassembly	IV3_integin_off_clu_rate = - (k3r + Paxillin_FAK * k3r_p) * IV3_integrin_clu
Net changes in $\alpha_v\beta_3$ integrin activation	D_IV3_integin = IV3_integin_on_rate + IV3_integin_off_rate - IV3_integin_off_clu_rate
Net changes in $\alpha_v\beta_3$ integrin clustering	D_IV3_integin_clu = IV3_integin_on_clu_rate + IV3_integin_off_clu_rate
$\alpha_5\beta_1$ integrin activation	I51_integin_on_rate = k2f * I51_integrin_ina
$\alpha_5\beta_1$ integrin deactivation	I51_integin_off_rate = - k2r * I51_integrin_a
$\alpha_5\beta_1$ integrin cluster assembly	I51_integin_on_clu_rate = (k4f + Paxillin_p * k4f_p) * I51_integrin_a
$\alpha_5\beta_1$ integrin cluster disassembly	I51_integin_off_clu_rate = - (k4r + Paxillin_FAK * k4r_p) * I51_integrin_clu
Net changes in $\alpha_5\beta_1$ integrin activation	D_I51_integin = I51_integin_on_rate + I51_integin_off_rate - I51_integin_off_clu_rate
Net changes in $\alpha_5\beta_1$ integrin clustering	D_I51_integin_clu = I51_integin_on_clu_rate + I51_integin_off_clu_rate
Src base autophosphorylation	Src_on_rate_base = k5f0 * Src_ina
Integrin-mediated autophosphorylation	Src_on_rate_int = k5f * Src_ina * IV3_integrin_clu
Dephosphorylation of pSrc	Src_off_rate_p = - k5r * Src_p
FAK-mediated pSrc phosphorylation	Src_on_rate = k6f0 * Src_p * FAK_p
Dephosphorylation of 3pSrc	Src_off_rate_3p = - k6r * Src_3p
Net changes in pSrc	D_Src_p = Src_on_rate_base + Src_on_rate_int + Src_off_rate_p - Src_off_rate_3p
Net changes in 3pSrc	D_Src_3p = Src_on_rate + Src_off_rate_3p
FAK autophosphorylation	FAK_on_rate_base = k7f0 * FAK_ina
Integrin-mediated autophosphorylation	FAK_on_rate_int = k7f * FAK_ina * I51_integrin_clu FAK_on_rate_int = k7f * FAK_ina * I51_integrin_a * F
Dephosphorylation of pFAK	FAK_off_rate_p = - k7r * FAK_p
Src-mediated pFAK phosphorylation	FAK_on_rate = k8f * FAK_p * Src_p
Dephosphorylation of 3pFAK	FAK_off_rate_3p = - k8r * FAK_3p
Net changes in pFAK	D_FAK_p = FAK_on_rate_base + FAK_on_rate_int + FAK_off_rate_p - FAK_off_rate_3p
Net changes in 3pFAK	D_FAK_3p = FAK_on_rate + FAK_off_rate_3p

Note that the red text represents the tensioned integrin activation of FAKY397.

Table S5. Equations describing negative feedback regulation.

Paxillin Description	Equations
Paxillin activation	Paxillin_on_rate = k10f * Paxillin_ina * (Src_p+ Src_3p)
Disassembly of pPaxillin/FAK complex	Paxillin_off_rate = - k10r * Paxillin_p
Net changes in pPaxillin	D_Paxillin_p = Paxillin_on_rate + Paxillin_off_rate - Paxillin_FAK_off_rate
pPaxillin/FAK complex formation	Paxillin_FAK_on_rate = k9f * Paxillin_p * (FAK_p + FAK_3p)
Disassembly of pPaxillin/FAK complex	Paxillin_FAK_off_rate = - k9r * Paxillin_FAK
Net changes in pPaxillin/FAK complex	D_Paxillin_FAK = Paxillin_FAK_on_rate + Paxillin_FAK_off_rate

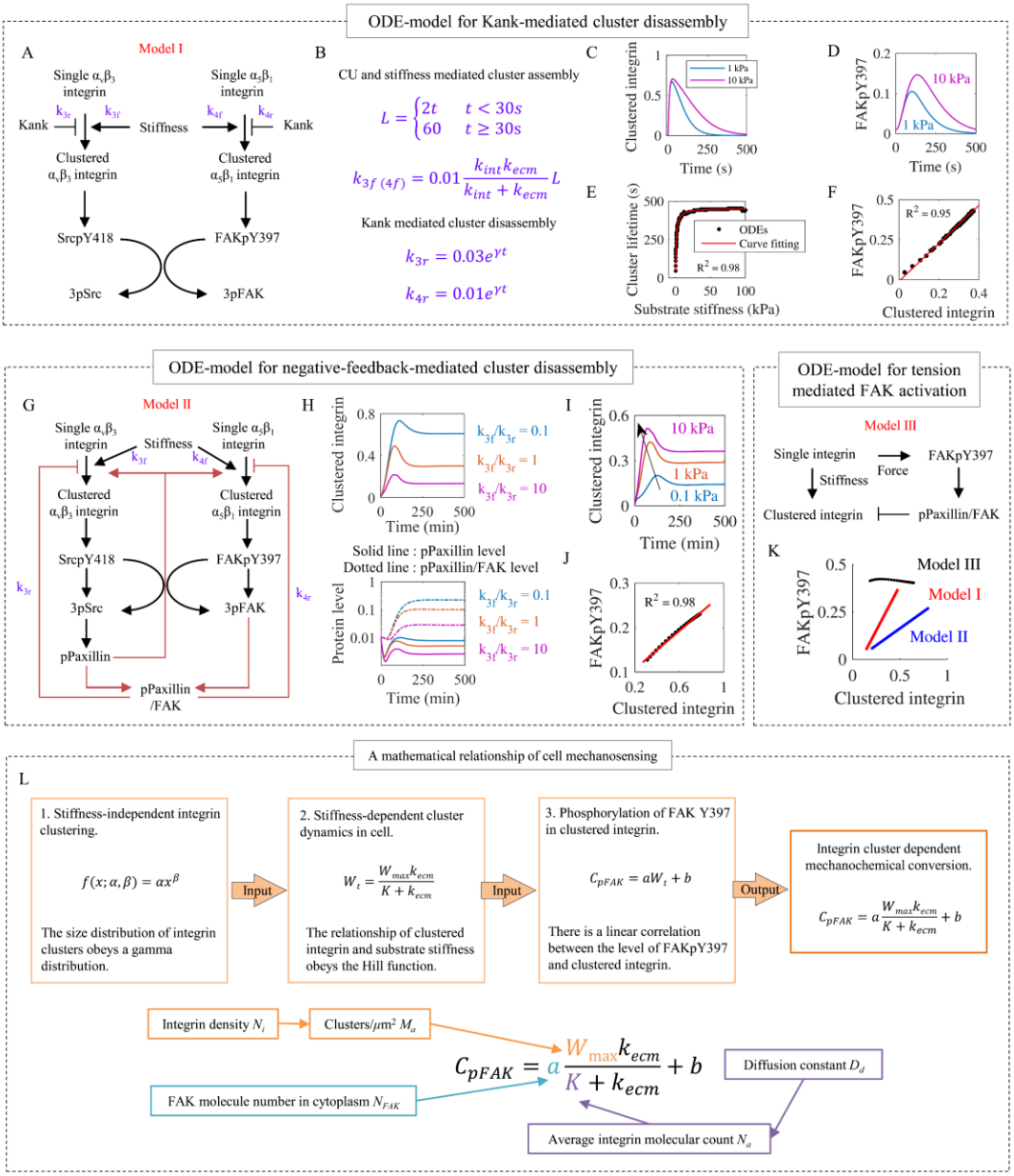

Fig. S1. Negative feedback ODE model. (A-B) The signaling network of the ODE-model for clustered-integrin-mediated FAKY397 activation. (C-D) The clustered integrin number and FAKY397 activation were enhanced on stiff substrata. (E) The relationship between integrin lifetime and substrate stiffness followed a Hill function. (F) FAKpY397 increased linearly with clustered integrins. (G) The signaling network of the ODE-model for paxillin negative feedback mediated integrin clustering. (H) The effects of FAK-mediated changes to integrin turnover rate on integrin clustering.

(I) The clustered integrin number was enhanced on the stiff substrate. (J) FAKpY397 increased linearly with clustered integrins. (K) Tension-mediated FAKY397 activation model. (L) The quantified relationship between substrate stiffness and FAKY397 activation. An algebraic expression is gotten to describe the stiffness-dependent mechanochemical conversion processes, i.e., the relationship between substrate stiffness and FAKpY397 number with the input factors: integrin density, FAK molecules in the cytoplasm and diffusion constant, which are distinct for different types of cells.

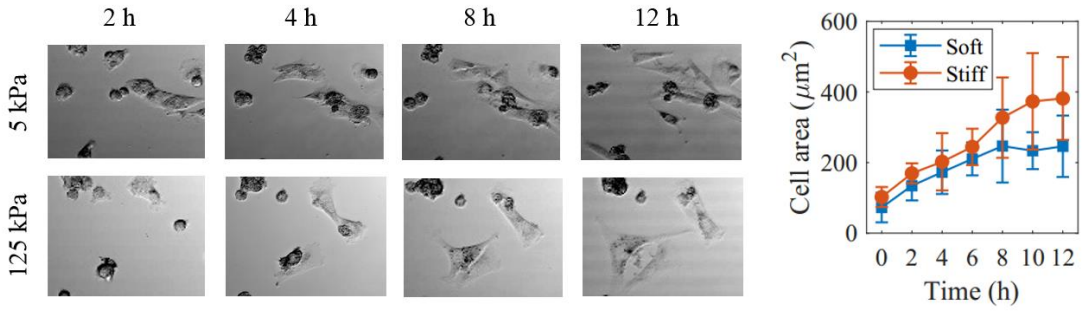

Fig. S2. Cell-spreading experiments. Experimental observations show that a steady plateau was reached after approximately 10 h, and that, as expected, cells spread more on stiffer substrata (stiff substrate: n = 20, 15, 23, 18, 10, 16, 20 cells for time = 0, 2, 4, 6, 8, 10, and 12 hours, respectively; soft substrate: n = 10, 12, 12, 12, 17, 15, 12 cells for time = 0, 2, 4, 6, 8, 10, and 12 hours, respectively).

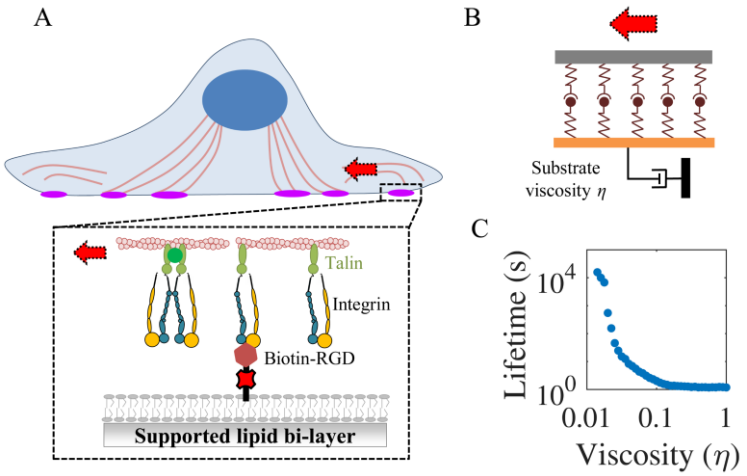

Fig. S3. The effect of substrate viscosity on the integrin cluster lifetime. (A) Focal adhesions were pulled towards the center of the cell by actomyosin contraction. (B) This motion was resisted by the viscous resistance of the lipid bilayer, modeled as a 1-dimensional viscosity, η. (C) The lifetime of bonds decreased sharply with increasing viscosity. The model for substrate viscosity contained an average of 50 integrin springs per cluster, consistent with the model for substrate stiffness.

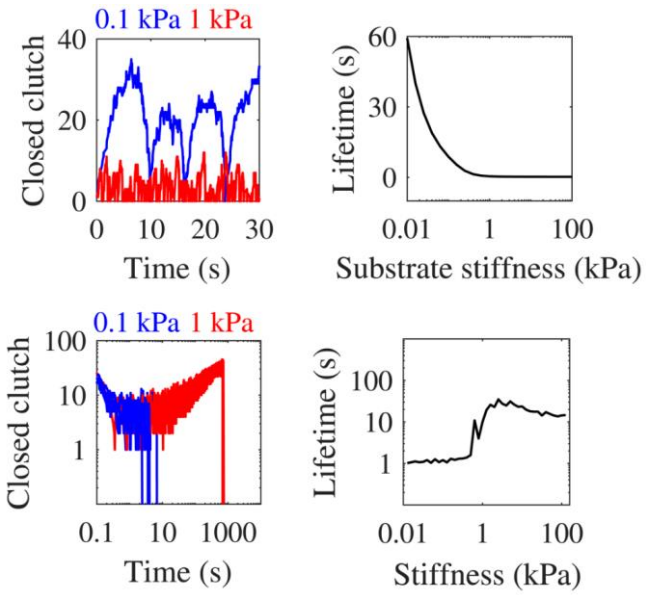

Fig. S4. The comparison of Odde's and our model. The comparison of the model of Odde, *et al.*, to the current model suggests that an assumption of homogeneity of tension across integrin molecules is appropriate for the cells studied in this article.

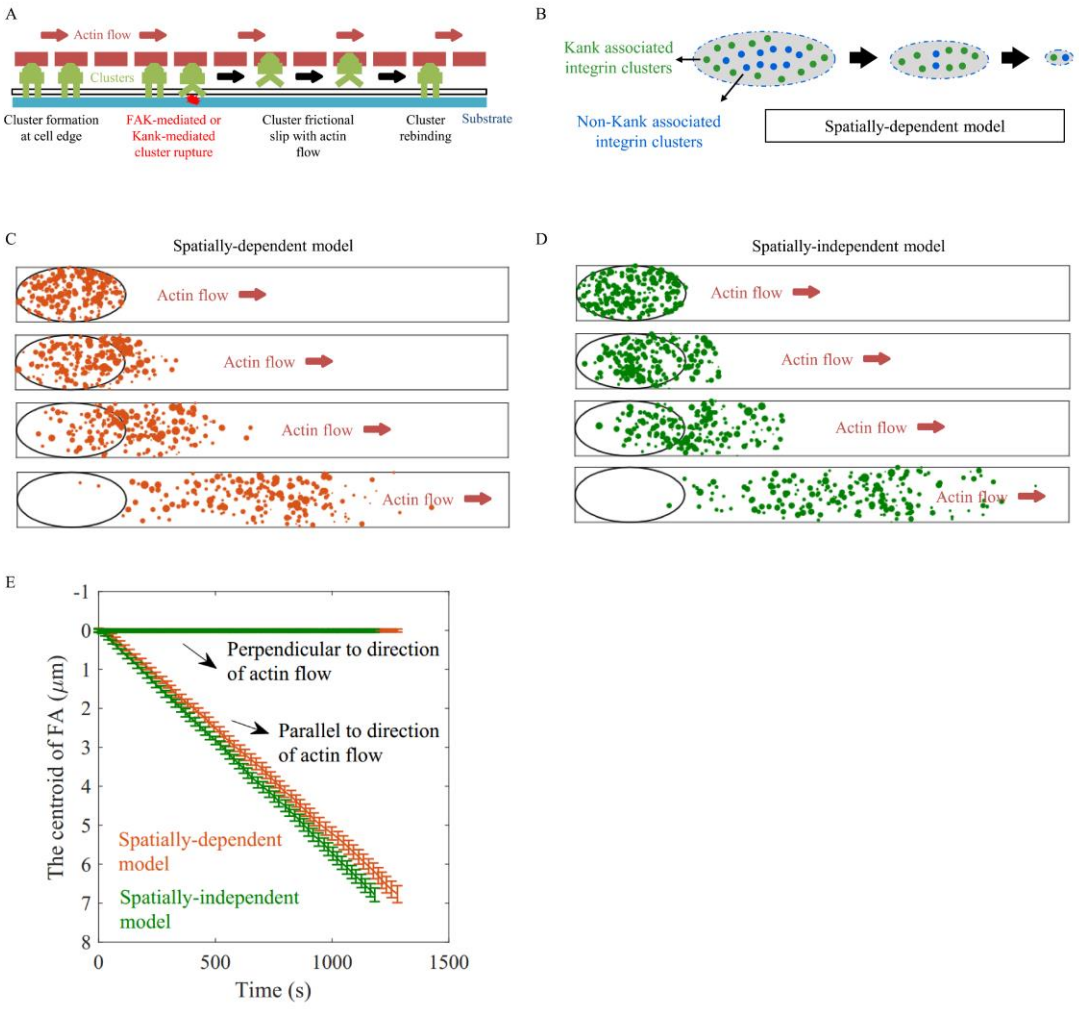

Fig. S5. Sliding assumption of intact FA. (A) Sliding model for an intact focal adhesion. (B) Disassembly of an intact focal adhesion by Kank. (C-E) The two computational implementations Kank-mediated cluster disassembly produced results that differed by only a few percent.